Int. J. Heat Mass Transfer. Vol. 14, pp. 467–482. Pergamon Press 1971. Printed in Great Britain

NATURAL CONVECTION IN A RECTANGULAR CAVITY TRANSIENT BEHAVIOR AND TWO PHASE SYSTEMS IN LAMINAR FLOW

J. SZEKELY and M. R. TODD†

Department of Chemical Engineering, State University of New York at Buffalo, Buffalo, New York 14214, U.S.A.

(*Received* 16 *January* 1970 *and in revised form* 18 *June* 1970)

Abstract—An analysis is presented for transient laminar natural convection in a rectangular cavity containing either one fluid or two immiscible liquids. The resultant differential equations were integrated numerically and computed results are presented for the transient streamline patterns and for the isotherms, for a variety of conditions including high, low and intermediate values of the Prandtl number.

The computed results agree with experimental data, both obtained in this study, and reported by other investigators. Such comparison is presented regarding temperature profiles, velocity profile, transient behavior and the onset of secondary flows.

NOMENCLATURE

c_p, specific heat;
D, width of the enclosure;
g, gravitational constant acting in the minus x direction;
Gr, Grashof number = $(g\beta\Delta T^* D^3)/\nu^2$;
Gr_x, local Grashof number = $(g\beta\Delta T(x^*) \cdot x^{*3})/\nu^2$;
$h(x^*)$, local heat-transfer coefficient = $q(x^*)/\Delta T^*$;
$h''(x^*)$, local heat-transfer coefficient based on the temperature difference between the hot wall and the vertical centerline of the slot;
k, thermal conductivity;
L, height of the enclosure;
Nu, mean Nusselt number;
Nu_x, local Nusselt number;
p, pressure;
p_i, initial pressure in static isothermal fluid;
p', pressure changes due to density variations and fluid motion;
Pr, Prandtl number = $\nu/\varkappa$;
$q(x^*)$, local heat flux;
Ra, Rayleigh number = $Gr \cdot Pr$;
t, time;
T, temperature;
T_i, initial temperature;
T_c, cold wall temperature;
T_h, hot wall temperature;
u_x, u_y, velocity in the x and y directions respectively;
U, reference velocity in the x direction = $\varkappa L/D^2$;
x, vertical co-ordinate measured upward from the lower left-hand corner of the enclosure;
X, reference distance in the x direction = L;
x_i, vertical distance from the origin to the interface;
y, horizontal co-ordinate measured from the lower left-hand corner of the enclosure.

Greek symbols

β, temperature coefficient of cubical expansion;

† Present address: Shell Development Co., Houston, Texas 77001.

ΔT, temperature difference $= T_h - T_c$;
ΔT^*, temperature difference $= T_h^* - T_c^*$;
$\Delta T(x^*)$, temperature difference $= T_h^* - T^*(x^*, D/2)$;
ξ, vorticity, defined in equation (8);
$\varkappa$, thermal conductivity:
ν, kinematic viscosity $= \mu/\rho$;
ρ, density;
ρ_i, initial density of the isothermal fluid in the enclosure;
ψ, stream function.

* denotes dimensional quantities.
Subscripts a and b refer to phases a and b respectively, in the two phase systems.

1. INTRODUCTION

NATURAL convection in confined systems has been extensively studied. The early experimental work, starting with Nusselt, was mainly concerned with the establishment of empirical correlations for the heat-transfer coefficients for systems contained between two parallel vertical plates [1–3]. More recently Eckert and Carlson [4] provided useful information on the temperature profiles and hence on the circulation pattern. Elder [5] investigated the velocity and the temperature profiles in narrow slots, and arrived at the criteria for the establishment of secondary and tertiary flows.

Regarding the theoretical work, the essentially asymptotic analyses of Elder [5], Batchelor [6] and Gill [7] were followed by the discussion of truly multidimensional problems, requiring the use of numerical techniques.

The application of numerical techniques and digital computation for natural convection problems was pioneered by Churchill and Wilkes [8], who studied the steady state and transient behavior of fluids contained in rectangular cavities. In subsequent work Aziz and Hellums [9] considered three dimensional systems heated from below whereas work by Elder [10], de Vahl Davis [11], and Newell and Schmidt [12] was concerned with steady state systems.

It is noted that in the majority of cases the experimental and analytical investigations were carried out independently of each other and with few exceptions little effort has been made to attempt a direct comparison between prediction and measurements.

A recent paper by McGregor and Emery [13] constitutes a notable exception, as these authors have obtained very good agreement between prediction and measurement for moderate to large Prandtl numbers, in the steady state regime.

It is noted that transient behavior received much less attention (although in many instances the steady state solutions were obtained from a transient formulation) and in particular no comparison is available between prediction and measurement in the unsteady state.

Another point that may be raised is that in the majority of cases the principal motivation was a better understanding of the heat-transfer process with application to problems such as thermal insulation, thermosyphons, and the cooling of nuclear reactors.

Natural convection plays a very important role in materials processing at high temperatures where agitation by other means is impracticable, or where the existence of temperature gradients (and the absence of forced flow) is an inherent characteristic of the system. Examples for such operations are the manufacture of glass in reverbatory furnaces, various slag–metal reactions and the circulation of liquid metals in solidifying ingots. These problems have been hardly explored up to the present.

The work to be reported here was undertaken with a dual objective in mind:

(a) To perform the analysis of steady and unsteady natural convection in systems relevant to problems in materials processing such as the transient development of the flow field at low Prandtl numbers (casting applications) and the behavior of two phase system , relevant to slag–metal reactions.

(b) To compare the computed results with experimental data produced both by other investigators and the present investigation.

While the experimental and computational techniques used in this study are analogous to those employed in recent investigations, the actual results to be presented are thought to complement available information on natural convection in confined systems.

Regarding the organization of the paper, the formulation is given in Section 2, some computational details are described in Section 3, and typical computed results are shown in Section 4. The experimental procedure is described in Section 5 and a comparison between measurement and prediction is presented in Section 6.

2. FORMULATION

The one phase system

Let us consider a rectangular slot of height L, of width D and of infinite extent in the z direction, as sketched in Fig. 1.

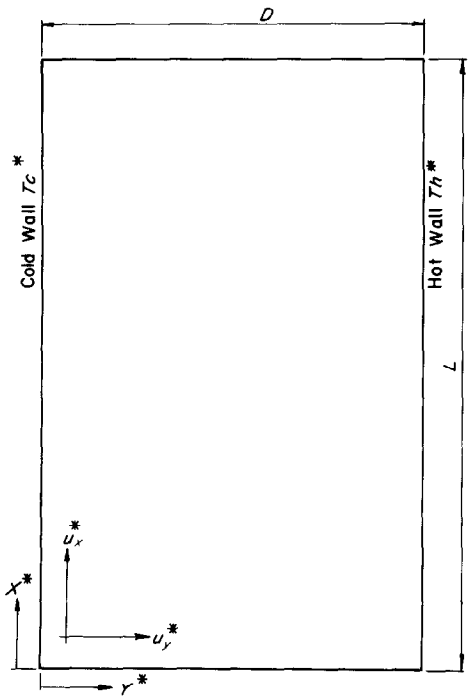

FIG. 1. Schematic representation of the one phase system.

Initially, let the fluid be at rest, and at a temperature T_i^*,† and for subsequent times let the vertical walls be kept at the constant temperatures T_c^* and T_h^*.

The upper and lower surfaces may be considered to have either fixed temperature profiles (corresponding to some experimental results) or, these surfaces may be considered to be insulated.

The problem is to find the time and spatial dependence of the velocities and the temperatures within the system.

The following assumptions are made:

(i) The fluid is considered to be Newtonian.
(ii) The physical properties, such as viscosity, density, thermal conductivity, etc., are assumed to be independent of temperature, and evaluated at T_i^*, with the exception of the contribution of the temperature dependent density to the buoyancy forces.
(iii) Laminar flow throughout.

While all these assumptions are restrictive, they are thought to represent quite a broad spectrum of practical situations.

The problem may now be stated by expressing the continuity and the heat and momentum balance equations, together with the appropriate initial and boundary condition. Thus we have:

$$\frac{\partial u_x^*}{\partial x^*} + \frac{\partial u_y^*}{\partial y^*} = 0 \tag{1}$$

(continuity)

$$\frac{\partial T^*}{\partial t^*} + u_x^* \frac{\partial T^*}{\partial x^*} + u_y^* \frac{\partial T^*}{\partial y^*} = \varkappa\left[\frac{\partial^2 T^*}{\partial x^{*2}} + \frac{\partial^2 T^*}{\partial y^{*2}}\right] \tag{2}$$

(energy balance)

Finally the two components of the momentum balance equation may be written as [14]:

† Dimensional variables are generally denoted by asterisks in the text.

$$\frac{\partial u_x^*}{\partial t^*} + u_x^* \frac{\partial u_x^*}{\partial x^*} + u_y^* \frac{\partial u_x^*}{\partial y^*} = g\beta[T^* - T_i^*] - \frac{1}{\rho_i}\frac{\partial p^*}{\partial x^*} + \nu\left[\frac{\partial^2 u_x^*}{\partial x^{*2}} + \frac{\partial^2 u_x^*}{\partial y^{*2}}\right]$$

and

$$\frac{\partial u_y^*}{\partial t^*} + u_x^* \frac{\partial u_y^*}{\partial x^*} + u_y^* \frac{\partial u_y^*}{\partial y^*} = -\frac{1}{\rho_i}\frac{\partial p^*}{\partial y^*} + \nu\left[\frac{\partial^2 u_y^*}{\partial x^{*2}} + \frac{\partial^2 u_y^*}{\partial y^{*2}}\right]. \quad (3)$$

The initial and boundary conditions have to express the physical constraints imposed on the system, namely that the initial temperature is uniform, the initial velocity is zero, the velocity is zero at the boundaries, and that the temperatures are specified at the bounding surfaces.

These are readily stated, available elsewhere [15], and therefore will not be reproduced here.

In order to express equations (1)–(3) in a form more suitable for solution by numerical techniques, let us introduce ξ^*, the vorticity vector and ψ^*, the stream function. For a two dimensional system, to be considered here, these are defined as follows:

$$\xi^* = \frac{\partial u_y^*}{\partial x^*} - \frac{\partial u_x^*}{\partial y^*} \quad (4)$$

and

$$u_x^* = \frac{\partial \psi^*}{\partial y^*}; \qquad u_y^* = -\frac{\partial \psi^*}{\partial x^*}. \quad (5)$$

Here ξ and ψ are related as follows:

$$\xi^* = -\left[\frac{\partial^2 \psi^*}{\partial x^{*2}} + \frac{\partial^2 \psi^*}{\partial y^{*2}}\right]. \quad (6)$$

Furthermore, for the purpose of computation it is desirable to express the governing equations in a dimensionless form. Let us introduce the following dimensionless variables:

$$\left.\begin{aligned} x &= \frac{x^*}{L}; \quad y = \frac{y^*}{D}, \quad t = \frac{t^*\varkappa}{D^2} \\ u_x &= \frac{u_x^* D^2}{\varkappa L}; \quad u_y = \frac{u_y^* D}{\varkappa} \\ \psi &= \psi^* \frac{D}{\varkappa L}; \quad \xi = \xi^* \frac{D^3}{\varkappa L} \\ \text{and} \quad T &= \frac{T^* - T_i^*}{T_h^* - T_c^*}. \end{aligned}\right\} \quad (7)$$

After some manipulation the governing equations may then be expressed as:

$$\frac{\partial T}{\partial t} + u_x \frac{\partial T}{\partial x} + u_y \frac{\partial T}{\partial y} = \left(\frac{D}{L}\right)^2 \frac{\partial^2 T}{\partial x^2} + \frac{\partial^2 T}{\partial y^2} \quad (8)$$

$$\frac{\partial \xi}{\partial t} + u_x \frac{\partial \xi}{\partial x} + u_y \frac{\partial \xi}{\partial y} = \left(\frac{D}{L}\right)^2 Pr \frac{\partial^2 \xi}{\partial x^2} + Pr \frac{\partial^2 \xi}{\partial y^2} - RaPr \frac{D}{L}\frac{\partial T}{\partial y} \quad (9)$$

where

$$\xi = -\left(\frac{D}{L}\right)^2 \frac{\partial^2 \psi}{\partial x^2} - \frac{\partial^2 \psi}{\partial y^2}. \quad (10)$$

Here equation (8) is the dimensionless form of the energy balance equation and equation (9) is the vorticity transport equation which combines the two components of the equation of motion.

The velocity boundary conditions are readily stated in terms of the stream function; it is noted that the conditions specifying a zero normal velocity component at the bounding surfaces are satisfied by requiring that the stream function be constant along the boundary.

Equations (8)–(10) represent a complete statement of the problem. For high values of the Prandtl number, the vorticity transport equation (9) simplifies to:

$$\left(\frac{D}{L}\right)^2 \frac{\partial^2 \xi}{\partial x^2} + \frac{\partial^2 \xi}{\partial y^2} = Ra\left(\frac{D}{L}\right)\frac{\partial T}{\partial y} \quad (11)$$

which may be put in the following form:

$$\left(\frac{D}{L}\right)^4 \frac{\partial^4 \psi}{\partial x^4} + 2\left(\frac{D}{L}\right) \frac{\partial^4 \psi}{\partial x^2 \partial y^2} + \frac{\partial^4 \psi}{\partial y^4} = -\left(\frac{D}{L}\right) Ra \frac{\partial T}{\partial y}. \quad (12)$$

Equation (12) is readily integrated by well-established, numerical techniques.

The two phase system

Let us consider the identical rectangular slot, described in the preceding section, but containing two immiscible fluids, separated by a horizontal interface. Let the upper and lower fluids be denoted by "b" and "a" respectively, and let the position of the interface be denoted by x_i^*, the dimensionless equivalent of which is $x_i \equiv x_i^*/L$.

The differential equations describing such systems will be almost identical to those given previously, but we shall require one set of equations for each phase.

The boundary conditions pertaining to the vertical walls will remain the same, but new boundary conditions will be required at the interface of the two immiscible liquids. On assuming that no deformation of the interface occurs (which seem reasonable for relatively low velocities) these have to express the continuity of the temperature, of the heat flux, of the velocity and of the momentum flux. In addition we must have that of the interface; the vertical velocity components are zero in both phases. Thus we have:

$$\left.\begin{aligned} &u^*_{xa}(x_i, y, t) = 0; \qquad u^*_{xb}(x_i, y, t) = 0 \\ &u^*_{ya}(x_i, y, t) = u^*_{yb}(x_i, y, t) \\ &\mu_a \frac{\partial u^*_{ya}}{\partial x^*}(x_i, y, t) = \mu_b \frac{\partial u^*_{yb}}{\partial x^*}(x_i, y, t) \end{aligned}\right\} \quad (13)$$

and

$$\left.\begin{aligned} &T_a(x_i, y, t) = T_b(x_i, y, t) \\ &k_a \frac{\partial T^*_a}{\partial x^*}(x_i, y, t) = k_b \frac{\partial T^*_b}{\partial x^*}(x_i, y, t) \end{aligned}\right\} \quad (14)$$

where subscripts "a" and "b" refer to phase a and b respectively.

3. THE TECHNIQUE FOR SOLUTION

The governing equations were put in a finite difference form and a spatial grid of 11 × 11 or 11 × 21 was established for the one fluid and two fluid systems, respectively.

The alternating direction implicit variant of the Crank–Nicholson procedure was used for vorticity transport equations, and the successive overrelaxation technique was employed for the integration of the stream equation.

The simultaneous solution of these three equations was accomplished by an iterative procedure, which contained the following main steps:

(1) At a given time, for known values of the temperature, velocity, vorticity and stream fields, the temperature is advanced by one time step, by using the alternating direction implicitly (A.D.I.) technique.†

(2) This first estimate of the temperature field is now used for obtaining a first estimate of the interior vorticity field, by using A.D.I.

(3) Then, we compute values of the stream function, by using a successive over-relaxation technique.

(4) From the stream function we compute the velocity components and the first outer loop is completed by calculating the vorticity at the boundaries, which satisfies: $u_x = u_y = 0$.

(5) The new values of the vorticity thus found at the boundaries, meets the physical criteria imposed by the boundary conditions, but is now "out of step" with the interior vorticity field. To overcome this difficulty, another iterative loop is

† Alternating direction implicit technique, as described in Peaceman and Rachford [16].

created, with a view of finding a vorticity distribution which satisfied simultaneously the vorticity transport equation and the boundary conditions on the stream equation.

(6) This iterative loop consisted in recalculating the vorticity and the stream function (and the temperature field) using the last value of the boundary vorticity, until two successive iterations agreed to within 0·1 per cent. The actual velocities used in these iterations were arithmetic averages of those computed on the "old" and the "new" time steps. The continued use of this procedure eventually yielded the steady state solution.

4. COMPUTED RESULTS

Some typical computed results are shown in Figs. 2–4. A more extensive set of computed curves is available in the thesis [15] on which this paper is based.

Figure 2 shows the behavior of a system with $Pr = 1$, $Gr = 5000$† and $L/D = 1$. Initially the fluid is stationary and the temperature field is uniform; at time = 0 both walls are raised to $T = +0{\cdot}5$, with the horizontal surfaces insulated. ($\partial T/\partial x = 0$ at $x = 0$, $x = 1$). Here the circulation rate has to pass through a maximum at some intermediate time as the fluid is, of course, stationary both initially, and on the attainment of the steady state. The streamlines and the isotherms corresponding to such an intermediate time are shown in Fig. 2a and 2b, respectively.

It is seen that the circulation pattern is composed of two countercurrent cells rather than having just one cell, as found for systems where the walls are kept at different temperatures.

Had the slot been cooled, rather than heated, the streamline pattern would have been identical but for the direction of the currents. The isotherms for this case would have been the mirror image, about the y axis, of those shown in Fig. 2b.

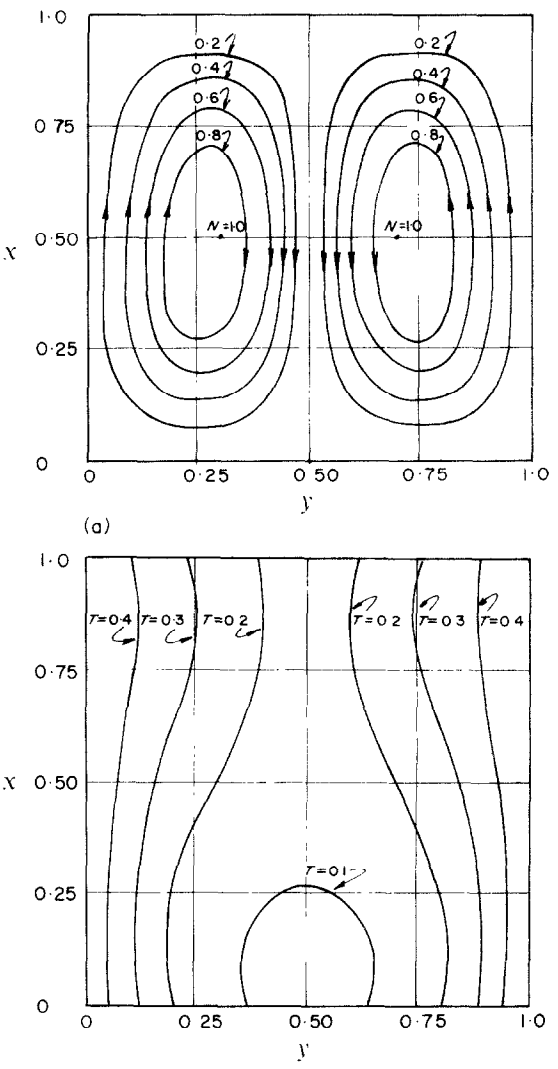

FIG. 2. Streamline patterns and isotherms for a system with $Gr = 5000$, $Pr = 1{\cdot}0$, $L/D = 1$, for $t > 0$, $T = +0{\cdot}5$ at $y = 0$ and at $y = 1{\cdot}0$ for $t > 0$.
(a) streamline pattern at $t = 0{\cdot}05$, the numbers on the curves denote the fractional value of ψ; $\psi_{max} = 2{\cdot}00$.
(b) isotherms at $t = 0{\cdot}05$.

If Fig. 3 we show the transient development of the stream and temperature field for a system with $L/D = 1{\cdot}0$, $Pr = 0{\cdot}02$ and $Gr = 5000$. Initially the fluid is stationary and the temperature field is uniform; then at time = 0 both

† Based on the temperature difference $T_h^* - T_l^*$.

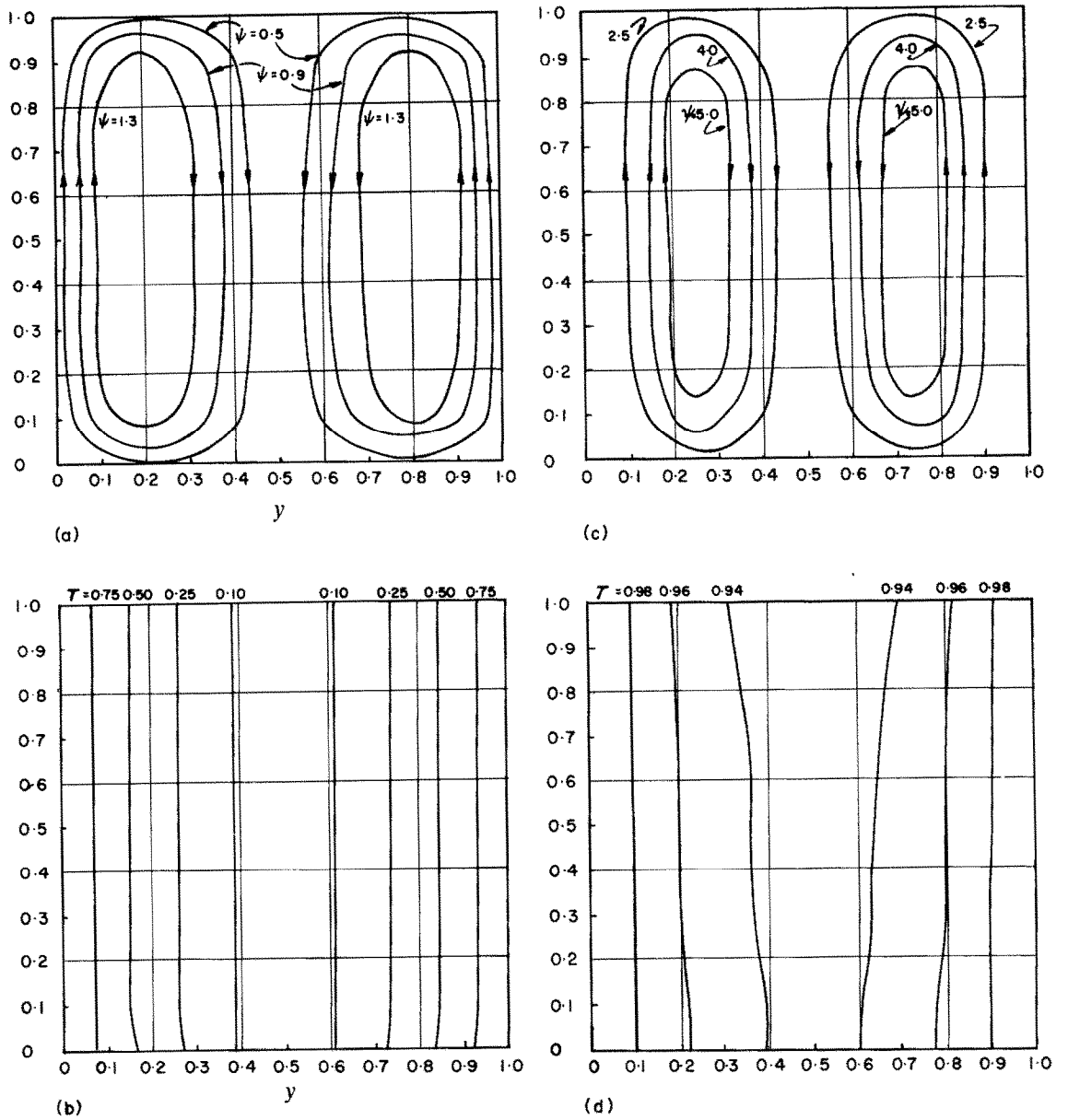

FIG. 3. Streamline patterns and isotherms for a system with $Gr = 5000$, $Pr = 0{\cdot}02$, $L/S = 1{\cdot}0$, where $T = +0{\cdot}5$ at $y = 0$ and $y = 1$, for $t > 0$. The upper and lower faces are insulated.

(a) streamlines at $t = 0{\cdot}025$; the numbers on the curves denote 4×10^2.

(b) isotherms at $t = 0{\cdot}025$.

(c) streamlines for $t = 0{\cdot}300$.

(d) isotherms for $t = 0{\cdot}300$.

vertical walls are suddenly raised to $T = +0{\cdot}5$.

Inspection of Figs. 3a–3c shows, that for this system, which corresponds to liquid metals, both the stream and temperature fields are established very rapidly. An unusual feature of this situation, which is characteristic of low

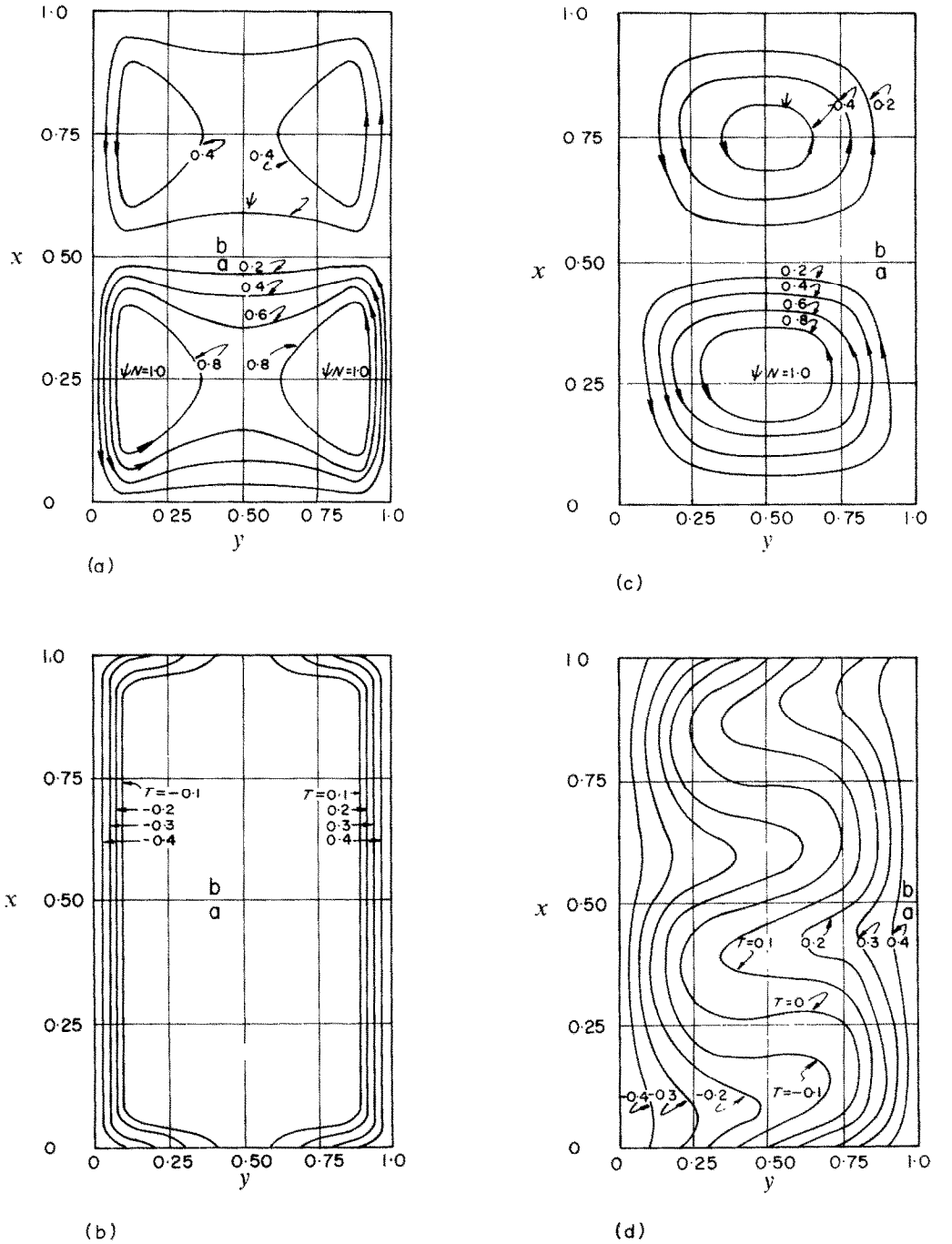

FIG. 4. The transient development of streamlines and isotherms for a two phase system.
Fluid a: $Gr = 20000$, $Pr = 2{\cdot}0$.
Fluid b: $Gr = 20000$, $Pr = 1{\cdot}0$.
$L/D = 2{\cdot}0$; for $t > 0$, $T = -0{\cdot}5$ at $y = 0$ and $T = +0{\cdot}5$ at $y = 1{\cdot}0$.
(a) streamline patterns at $t = 0{\cdot}0025$: $\psi_{max} = -1{\cdot}40$.
(b) isotherms at $t = 0{\cdot}0025$.
(c) streamline patterns at $t = 0{\cdot}1$, $\psi_{max} = -7{\cdot}56$.
(d) isotherms at $t = 0{\cdot}1$.

Prandtl numbers, is the fact the extensive fluid circulation remains even when the temperature field is almost uniform.

It follows that in this case the stream field decays much slower than the non-uniformities in the temperature. As identical considerations would apply to cooling and this behavior is of considerable practical importance as it explains the extensive circulation occurring in solidifying ingots, even under conditions, where all the superheat has been removed.

A comparison of Figs. 2 and 3 shows the expected behavior, namely that the circulation has a significant effect on the shape of the isotherms at $Pr = 1{\cdot}0$, whereas the temperature field is much less affected by the fluid motion at $Pr = 0{\cdot}02$.

Finally, Fig. 4 shows computed streamlines and isotherms for a two fluid system. Initially both fluids are at the same, uniform temperature, and from $t = 0$, the l.h.s. and r.h.s. walls are maintained at dimensionless temperatures of $-0{\cdot}5$ and $+0{\cdot}5$, respectively. The property values were so chosen, that the Prandtl number in the lower phase is twice that in the upper phase, whereas the Grashof numbers are equal in both phases.

The circulation patterns are found to be similar to those in the single fluid systems; the higher value of Pr (or rather Ra) in phase (a) causes a stronger circulation here, but the higher thermal conductivity in the upper phase causes a more rapid development of the temperature field.

5. APPARATUS AND EXPERIMENTAL PROCEDURE

The apparatus

The apparatus was so constructed to allow the study of an essentially two dimensional flow and temperature field both under steady state and unsteady state conditions.

The major components of the apparatus consisted of a rectangular enclosure which held the working fluid(s), a control system that maintained the wall temperatures at desired levels and the probe, together with its associated transport mechanism, and recorders used to measure and record the temperatures within the system. A schematic diagram of the apparatus is shown in Fig. 5. The rectangular slot, holding

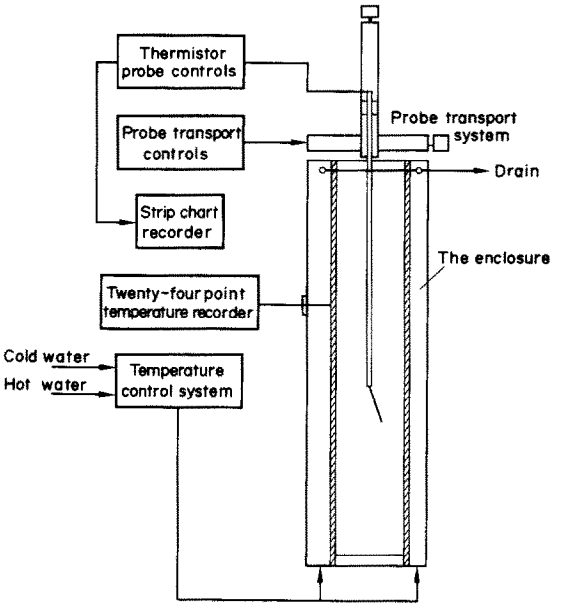

FIG. 5. Schematic representation of the apparatus.

the fluid(s) was 36 in. high, 24 in. long and 4·8 in. wide. The two opposing vertical plates which constituted the principal walls, were made of copper, whereas the "side walls" were made of plate glass, so as to allow visual observations. Water jackets were attached to the copper walls which contained fittings for the water inlet and outlet, and also for the thermocouple probes. The temperature of each copper wall was maintained to within 0·1°C of the desired value by circulating water of appropriate temperature through the jackets. The temperature of the circulating water streams was controlled by proportioning the feed from two constant temperature reservoirs. The temperature of the copper walls was measured at 24 locations, by chromel–alumel thermocouples, connected to a multichannel recorder.

The temperature within the fluid was measured by a thermistor probe, the shaft of which was mounted on a motorized worm gear mechanism, the programming of which allowed the "automatic" horizontal and vertical traverse of the system.

The materials used

The fluids used had to meet the criteria for immiscibility and their physical properties had to be such that Rayleigh numbers of the order of 10^4–10^5 could be obtained in the apparatus, at accurately measurable temperature differences. This upper limit of the Rayleigh number was dictated by both observations [3] and predictions that above $Ra \simeq 2 \times 10^4$, *secondary flows* would begin to occur.

From a practical viewpoint these criteria meant that we were looking for a pair of immiscible fluids which were viscous and had moderate coefficients of thermal expansion.

The property values of the two fluids selected are given in Table 1.

Table 1. Property values of the fluids used

Property	Numerical value	
	Fluid (a) Therminol Fr-3 (Monsanto)	Fluid (b) Ambiflow H813 (Dow Chemical Co.)
Specific heat C_p [cal/g°C]	0·239	0·45
Coefficient of thermal expansion β [°C^{-1}]	$1{\cdot}98 \times 10^{-4}$	$7{\cdot}6 \times 10^{-4}$
Thermal conductivity k [cal/s cm°C]	$2{\cdot}36 \times 10^{-4}$	$4{\cdot}92 \times 10^{-4}$
Viscosity μ, [p]	250·0	19·0
Density, ρ [g/cm^3]	1·54	1·06
Thermal diffusivity κ, [cm^2/s]	$6{\cdot}36 \times 10^{-4}$	$1{\cdot}03 \times 10^{-3}$
Pr	$2{\cdot}5 \times 10^5$	$1{\cdot}75 \times 10^4$

Experimental procedure

All the experimental runs were carried out using the two phase system, although in the majority of cases measurements were made only in one of the phases.

In a given series of experimental runs the container was filled with the heavier of the two liquids (Therminol) to a depth of about 8 in. The lighter fluid (Ambiflow) was then carefully poured on top of the Therminol, bringing the total depth to about 16 in.

In the transient runs the entire system was brought to a stationary isothermal state by setting the wall temperature to the same values and by allowing some 24 h for the system to attain thermal equilibrium. The attainment and approach to thermal equilibrium was measured by taking horizontal temperature profiles at various vertical levels.

It was found that even small temperature changes in the room, in which the apparatus was located, had a significant effect on the temperature distribution in the vicinity of the top and bottom surfaces. These effects were, however, confined to a finite distance from the horizontal bounding surfaces (say 1–4 in.) and did not affect the transient response of the system, as measured near the horizontal center line of the fluid layer. In the comparison of experimental measurements with predictions in the steady state, appropriate allowance was made for heat exchange between the fluid and the environment through the horizontal boundaries; this was done by the adjustment of the boundary conditions at $x = 0$ and $x = 1$ in the computation.

On the attainment of steady, isothermal conditions, one of the wall temperatures was raised to the desired value; $(T_h^* - T_c^*)$ was usually of the order of 3–5°C, and the traverse of the probe was initiated. When steady state was reached, as evidenced by the temperature recordings, the recorders and the probe mechanism were shut down. Then one more temperature profile was taken 24 h later, to ensure that steady state had indeed been established.

Under the experimental conditions the attainment of steady state took usually about 7 h, and

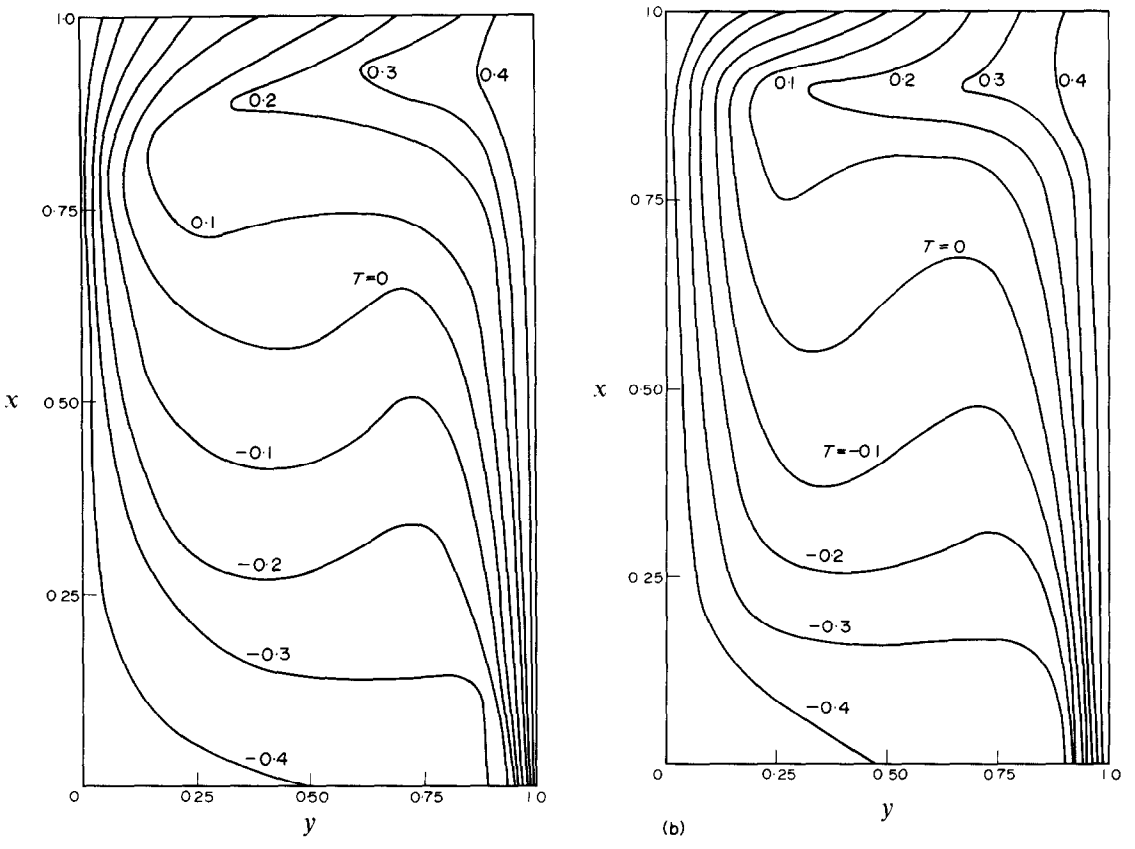

FIG. 6. A comparison of experimental and computed steady state isotherms for $L/D = 1{\cdot}83$, $Ra = 8{\cdot}2 \times 10^3$ and $Pr = 2{\cdot}45 \times 10^3$; $T = -0{\cdot}5$ at $y = 0$, $T = +0{\cdot}5$ at $y = 1$; $T = -0{\cdot}5 + y$ at $x = 1$, and $T = -0{\cdot}4$ at $x = 0$.
(a) Experimental isotherms.
(b) Computed isotherms.

about 3 h were required for the fluid temperature at the center to reach 63 per cent of its final, steady value. Both these times were quite long, compared with the time taken to establish a new, steady wall temperature, which required about 6 min. Thus the change in the wall temperature could be regarded as a stepwise process in comparison to the time scale of convective transfer.

6. COMPARISON OF THE EXPERIMENTAL RESULTS WITH PREDICTIONS

Figure 6a shows steady state isotherms obtained experimentally for $L/D = 1{\cdot}83$, $Ra = 8{\cdot}2 \times 10^3$ and $Pr = 2{\cdot}45 \times 10^5$; the corresponding computed isotherms, for identical values of L/D, Ra and $Pr = \infty$ are shown in Fig. 6b. The close agreement between the experimental and the computed profiles is readily apparent.

It is noted that for the experimental conditions the horizontal temperature profile at the upper boundary was nearly linear, whereas the temperature profile at the lower boundary was approximately constant, i.e.

$$T(1, y) \simeq -0{\cdot}5 + y \tag{15}$$

and

$$T(0, y) \simeq -0{\cdot}4. \tag{16}$$

This temperature distribution resulted from

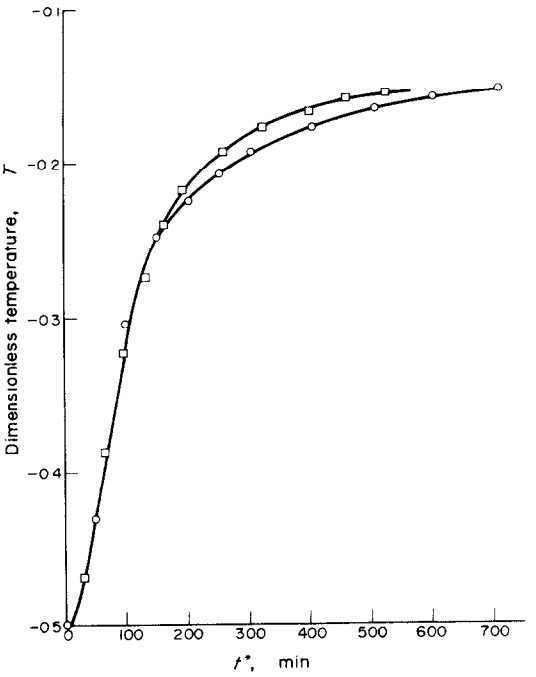

FIG. 7. A comparison of the predicted and measured time dependence of temperature at a given location for a system: $L/D = 1{\cdot}83$, $\varkappa = 1{\cdot}03 \times 10^{-3}$ cm^2 s
◯ Experimental data for $Ra = 1{\cdot}25 \times 10^5$.

the fact that for this particular experimental run the temperature of the environment was lower than that of either wall. The experimentally determined temperature profiles, at the boundary, as given by equations (15) and (16) were used as the boundary conditions in the computation.

It is of interest to compare measurement and prediction in the transient regime. This is done in Fig. 7 showing a plot of the dimensionless temperature against time in the "Ambiflow" fluid, at a location at 1·6 in from the cold wall and at the horizontal centerline, for $L/D = 1{\cdot}83$, and $Ra = 1{\cdot}25 \times 10^5$. The experimental data are denoted by the circles, and the computed data for $Ra = 6 \times 10^4$† are represented by the

† The legitimacy of using Ra in conjunction with a Prandtl number may be queried: it is noted, however, that for this asymptote the vorticity transport equation is written as:

$$(L/D)\frac{\partial^2 \xi}{\partial x^2} + \frac{\partial^2 \xi}{\partial y^2} = Ra(D/L).\frac{\partial T}{\partial y},$$

which does contain Ra.

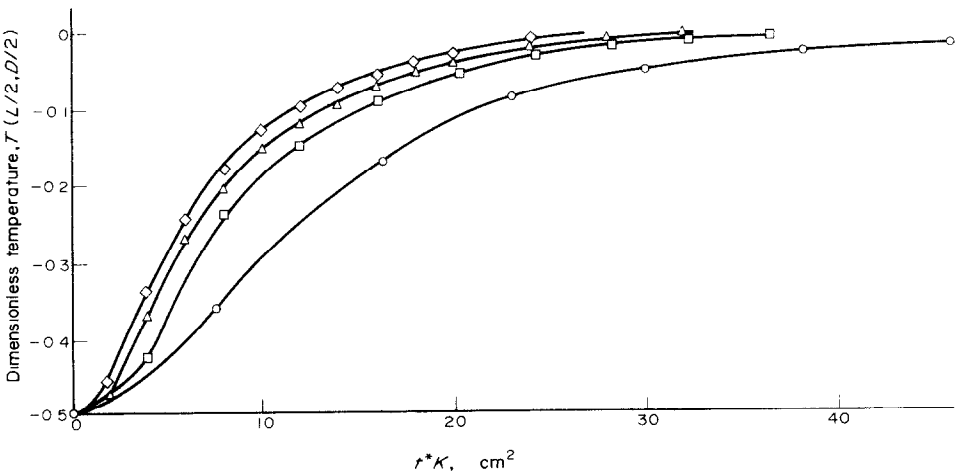

FIG. 8. Plot of the computed fluid temperature at the center of the cavity against $t \times \varkappa$ showing the effect of the Rayleigh number.

Legend:
◯ $Ra = 4000$.
□ $Ra = 16000$.
△ $Ra = 40000$.
◇ $Ra = 60000$.

squares; it is seen that good agreement exists between the computed and the measured data.

The fact that the value of Ra for the computed data was about half of that corresponding to the experimental conditions, deserves comment. The infinite Prandtl number asymptote was used for the computation, and for the numerical procedure used, $Ra = 6 \times 10^4$ was the maximum value which still gave a stable solution.

The error introduced by not matching the Rayleigh number exactly in the assessment of the transient temperature profile, is, however rather less than what one might expect.

To illustrate this point, Fig. 8 shows a plot of the computed dimensionless temperature at the center of the slot, against the product (dimensionless time × thermal diffusivity) with the Rayleigh number as a parameter. These calculations were performed, by using the infinite Prandtl number asymptote. It is seen that within the range $16000 < Ra < 60000$ the response of the system is not markedly affected by the value of the Rayleigh number. This finding is in itself of interest and may be regarded as a supporting argument for the procedure used in the comparison shown in Fig. 7.

In Fig. 9 there is shown a plot of the steady state temperature field for the two fluid system; dimensional spatial coordinates are used but the isotherms are represented in a dimensionless form. The hot and the cold walls were kept at 17·5 and 15°C respectively; the Rayleigh numbers corresponding to this temperature difference were $1{\cdot}74 \times 10^5$ and 8200 respectively. The isotherms shown in the lower layer are of a characteristic S shape which is consistent with one rotational cell, as discussed earlier.

The isotherms appearing in the upper fluid provide evidence for secondary flow, which is in agreement with Elder's experimental findings for single fluid systems.

It is noted that the presence of the upper fluid does not modify appreciably the temperature profile within the lower fluid, except for a region in the vicinity of the interface. This finding is in agreement with the computed results given in Section 4.

As the measurements made in this investigation concerned primarily the temperature field, it is of interest to compare the computed results

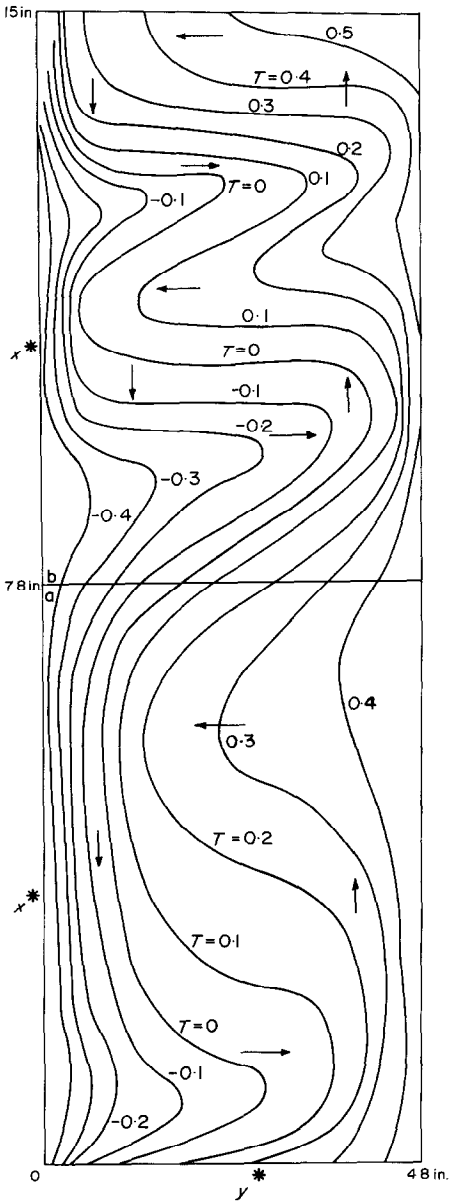

FIG. 9. Experimentally measured steady state isotherms for $T_c^* = 15°C$, $T_h^* = 17{\cdot}5$, $Ra_a = 1{\cdot}74 \times 10^5$, $Ra_b = 8200$.

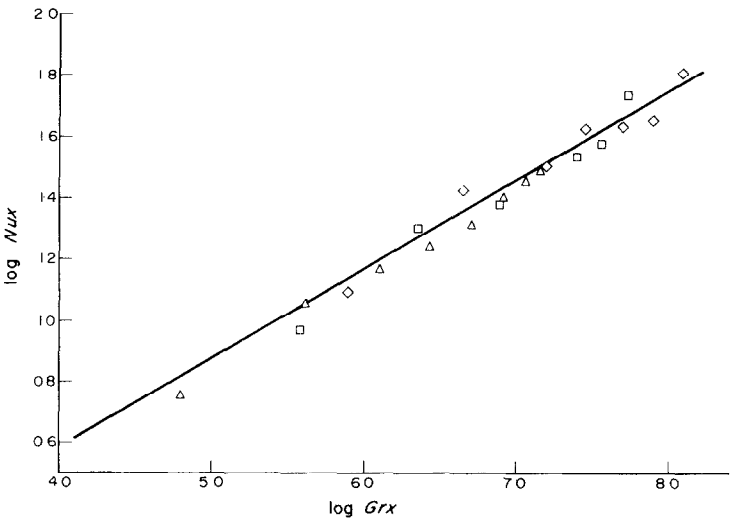

FIG. 10. Plot of the log of the local Nusselt number against the log of the local Grashof number showing the effect of Gr (based on the width of the cavity).

-- $Nu_x = 0{\cdot}231\ Gr_x^{0{\cdot}3}$.
△ $Gr = 10^4$
[] $Gr = 5 \times 10^4$, computed results.
· $Gr = 10^5$.

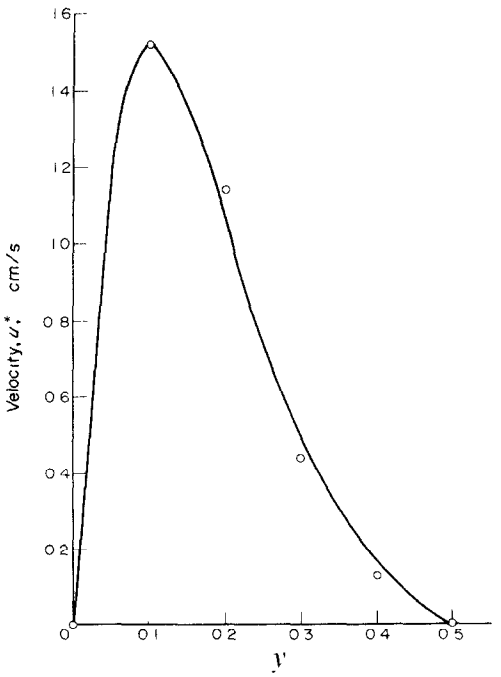

FIG. 11 A comparison of an experimentally measured velocity profile by Elder [6] with computed results. The conditions correspond to: $x = 0{\cdot}5$, $Ra = 4 \times 10^5$, $L/D = 18{\cdot}6$.

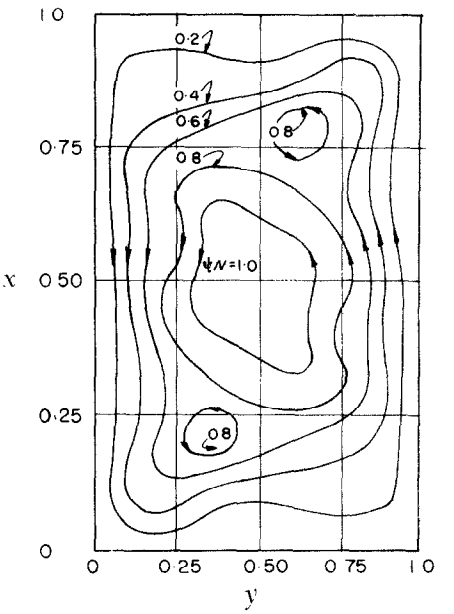

FIG. 12. The onset of secondary flows at high Rayleigh numbers. Streamline pattern for $Ra = 4 \times 10^5$, $Pr = 0{\cdot}733$, $L/D = 20$, $\psi_{max} = -9{\cdot}15$.

with data reported in the literature on heat transfer and on velocity profiles.

Figure 10 shows a plot of the local Nusselt number against the local Grashof number; the solid line represents an empirical correlation proposed by Eckert and Carlson, for air:

$$Nu_x = 0{\cdot}231\, Gr_x^{0{\cdot}3} \qquad (17)$$

whereas the discrete points represent the computed results. It is seen that the computed results are in good agreement with the experimental correlation. These results are relatively insensitive to Gr (i.e. the Grashof number, based on the width of the cavity) in apparent agreement with the findings of Eckert and Carlson.

Elder's work represents one of the few recent studies aimed at the measurement of velocity profiles in confined systems. Figure 11 shows excellent agreement between a measured velocity profile, depicted by a continuous line and the computed values (for identical physical conditions) denoted by the circles.

Finally, it is noted, that Elder reported that strong secondary cell activity occurred in his experiments, once the Rayleigh number exceeded 3×10^5. The computed results showed a similar trend, as seen in Fig. 12 illustrating the generation of secondary cells at $Ra = 4{\cdot}0 \times 10^5$.

While the mesh size used in the computation was too crude for the accurate definition of these secondary cells, the parallel between measurement and analysis is quite remarkable.

7. CONCLUDING REMARKS

The analysis is presented for transient natural convection in a rectangular cavity, holding either a single fluid, or two immiscible liquids.

The numerical techniques used were analogous to those employed by other investigators, however in the presentation of the results we stressed aspects of the problem which were relatively unexplored up to the present. Thus attention was paid to transient behavior, to two phase systems, and to the effect of a low Prandtl number.

The computed results were found to be in good agreement with both the experimental data obtained in the present study and with the measurements reported by other investigators.

The computed results for the unsteady state behavior of systems with low Prandtl numbers are relevant to casting problems and our findings explain observed behavior, that circulation currents may persist in molten metal systems long after the temperature field has attained its final uniform value.

ACKNOWLEDGEMENTS

In the initial phase of this work both authors were associated with the Metallurgy Department of Imperial College and then the project was supported by the Science Research Council. (U.K.) Subsequently the project was supported by the New York State Science and Technology Foundation under Grant No. S.S.F. 7(10).

In addition the authors wish to thank Dr. Stephen Margolis of S.U.N.Y. for helpful discussions.

REFERENCES

1. W. Nusselt, V.D.K., Nos. 63, 64, 68 (1909).
2. E. Schmidt, Heat transfer by natural convection, *Proc. Int. Heat Transfer Conf.*, Am. Soc. Mech. Engrs, xxix (1961).
3. M. Jakob, *Heat Transfer*, Vol. 1. John Wiley, New York (1949).
4. E. R. G. Eckert and W. O. Carlson, Natural convection in an air layer enclosed between two vertical plates with different temperature, *Int. J. Heat Mass Transfer* **2**, 106–120 (1961).
5. J. W. Elder, Laminar free convection in a vertical slot, *J. Fluid Mech.* **23**, part 1, 77–98 (1965).
6. G. K. Batchelor, Heat transfer by free convection across a closed cavity between vertical boundaries at different temperature, *Q. Appl. Math.* **12**, 209–233 (1954).
7. A. E. Gill, The boundary-layer regime for convection in a rectangular cavity, *J. Fluid Mech.* **26**, part 3, 515–536 (1966).
8. J. O. Wilkes and S. W. Churchill, The finite-difference computation of natural convection in a rectangular enclosure, *A.I.Ch.E. Jl* **12**, 161–166 (1966).
9. K. Aziz and J. D. Hellums, Numerical solution of the three-dimensional equations of motion for laminar natural convection, *Physics Fluids* **10**, 314–324 (1967).
10. J. W. Elder, Numerical experiments with free convection in a vertical slot, *J. Fluid Mech.* **24**, part 4, 823–843 (1966).
11. G. deVahl Davis, Laminar natural convection in an enclosed rectangular cavity, *Int. J. Heat Mass Transfer* **11**, 1675–1693 (1968).
12. M. E. Newell and F. W. Schmidt, Heat transfer by laminar natural convection within rectangular enclosures, *J. Heat Transfer*, **92**, 159 (1970).

13. R. K. McGregor and A. F. Emery, *J. Heat Transfer* **91**, 391 (1969).
14. J. D. Hellums and S. W. Churchill, Dimensional analysis and natural circulation, *Chem. Engng Prog. Symp. Ser.* **57**, No. 32, 75–80 (1960).
15. M. R. Todd, Transient natural convection in confied two phase systems, Ph.D. thesis, State University of New York at Buffalo (1969).
16. D. W. Peaceman and H. H. Rachford, The numerical solution of parabolic and elliptic differential equations, *J. Soc. Ind. Appl. Math.* **3**, 28–41 (1955).

CONVECTION NATURELLE DANS UNE CAVITÉ RECTANGULAIRE

Résumé—On analyse le cas d'une convection naturelle laminaire transitoire à l'intérieur d'une cavité rectangulaire contenant soit un fluide, soit deux liquides non miscibles. Les équations aux dérivées partielles sont intégrées numériquement et les résultats obtenus sont présentés en configurations de lignes de courant transitoires et d'isothermes, ceci pour une variété de conditions renfermant des valeurs hautes, basses et intermédiaires du nombre de Prandtl. Les résultats du calcul s'accordent avec les résultats expérimentaux obtenus dans cette étude et avec ceux rapportés par d'autres chercheurs. Une telle comparaison est présentée concernant les profils de température, de vitesse, le comportement transitoire et l'existence d'écoulements secondaires.

FREIE KONVEKTION IN EINEM RECHTECKIGEN BEHÄLTER

Zussammenfassung—Es wird eine Analyse gegeben für instationäre, freie Konvektion in einem rechteckigen Behälter, der entweder ein Fluid oder zwei nichtmischbare Flüssigkeiten enthält. Die sich daraus ergebenden Differentialgleichungen werden numerisch integriert. Ergebnisse werden angegeben für instationäre Stromlinienbilder und Isothermen unter einer Vielzahl von Bedingungen, einschliesslich hoher, niedriger und mittlerer Werte von Prandtl-Zahlen.

Die berechneten Ergebnisse stimmen mit den experimentellen Daten überein, die ebenfalls aus dieser Untersuchung stammen, über die jedoch andere Forscher berichten. Der Vergleich bezieht sich auf Temperaturprofile, Geschwindigkeitsprofile, das instationäre Verhalten und das Einsetzen von Sekundärströmungen.

ЕСТЕСТВЕННАЯ КОНВЕКЦИЯ В ПРЯМОУГОЛЬНОЙ ПОЛОСТИ

Аннотация—Дан анализ неустановившегося ламинарного режима при естественной конвекции в прямоугольной полости, заполенной либо однородной жидкостью, либо двумя несмешивающимися жидкостями. Полученные дифференциальные уравнения численно проинтегрированы, и приводятся расчетные линии тока и изотермы при различных условиях, включая большие, малые и промежуточные значения чисел Прандтля.

Расчетные значения совпадают с экспериментальными данными, полученными как в этой работе, так и в работах, опубликованными другими исследователями. Такое сравнение сделано для профилей температуры, скорости, характеристик неустоявшегося режима и начала вторичных течений.